First online: 27 April 2017

Dynamic Characteristics and Rocking Response of a Byzantine Medieval Tower

Emmanouil-Georgios Kouris[*1]

Department of Civil Engineering, Aristotle University of Thessaloniki,
541 24, Thessaloniki, Greece

[*1]ekouris@civil.auth.gr

Abstract-**This investigation deals with the dynamic response of a Byzantine unreinforced masonry tower. The tower is located on Mount Athos and was erected in 1427. It was built to host the bells of Vatopedion Monastery and is 25 m tall. It has suffered several earthquakes during its history, and some restoration interventions have been applied. Firstly, the architectural characteristics are considered in the light of seismic events that hit the monument. Then, the modal characteristics are investigated using a linear analysis. Finally, the limit analysis is adopted to examine the behaviour of the tower up to collapse due to out-of-plane failure. A force-based and a displacement-based method are applied, and the respective capacities are converted into spectral quantities using properties of the first mode. Possible collapse mechanisms are considered in conjunction with the observed after-shock damage. The safety factor is derived comparing the capacity curves with the considered spectra.**

Keywords- Byzantine Tower; Modal Analysis; Out-of-Plane Collapse; Limit Analysis; Capacity Curves

I. INTRODUCTION

In this paper, the inelastic response of traditional unreinforced masonry (URM) towers against seismic loads is investigated. Their dynamic behaviour is examined up to the state of collapse. It is common knowledge that the main defect of URM walls is their low tensile strength; as a consequence, URM has the tendency to produce cracks in its body when subjected to seismic forces. Under gravitational forces, structural elements are mainly in compression, while the inertial forces produce principal stresses that are tensile in one of the main directions. This kind of cracks may also appear due to differential settlement of the soil. When a structure is cracked, and there is no other connection between the adjacent members, then the part of the structure that is isolated would appear a vibration which has the characteristics of rocking. This type of vibration is very frequent for URM towers and drives to out-of-plane collapse.

Towers made of URM subjected to inertial forces usually collapse due to the overturning of the most critical part because of the insufficient connection between adjacent structural members [1]. The uppermost part is particularly vulnerable to seismic loads when there are not sufficient connections between structural members. Other possible collapse mechanisms are connected with diagonal cracks or sometimes with vertical cracks. These cracks have the tendency to separate the integer construction in parts. The parts if not interconnected in any other way (e.g. tie rods) contribute to the development of a critical mechanism which will bring about collapse. The development of such a collapse mechanism involves the overturning of the most critical part. In these cases the critical part which tends to separate and fail out-of-plane presents a dynamic vibration relevant to that of a rocking rigid body about a constant point [2-4].

Firstly, the rocking response of rigid bodies is investigated, and the relations of dynamic vibration are extracted. Then, two methods are applied to assess the seismic capacity of the structure: (i) a method where the capacity is expressed in terms of forces (force based assessment), and (ii) a second one which expresses the seismic capacity in terms of displacements (displacement based assessment). The recent tension in the assessment of structural capacity coincides with the recent method based on displacements and not with the traditional one based on forces [5-7]. In this analysis, a combination of the two methods is applied to determine the capacity curve of the structure [8].

Both methods are based on the limit analysis of the considered collapse mechanism [4, 9, 10]. The integral structure is cracked due to seismic forces and separates into two or more parts which constitute the collapse mechanism. These parts interact one another with simple contact or developing friction forces. The elastic or inelastic strains of masonry bodies are very small with respect to the displacements and/or rotations due to rigid body mechanics. Therefore, they can be considered negligible and not taken into account. This assumption is valid for low to moderate vertical loads [11].

The current paper investigates the seismic capacity of a monumental URM tower comparing two different methods. The investigation of the rocking phenomenon is applied with two distinct methods. In the first method, the rocking is examined analytically, and the equations of vibration are extracted for the case of dynamic response. The capacity curves under the action of inertial forces are estimated assuming a variety of possible collapse mechanisms. The critical collapse mechanism(s) is identified among them as the one with the lowest capacity regarding displacements and shear forces. Hence, the critical collapse mechanism may involve more than one mechanism which sequentially becomes the critical one.

DOI: 10.5963/JCES0601002

II. STATE OF THE ART

Recent earthquakes have shown that slender structures are prone to out-of-plane failures [12]. Limit analysis has been proposed as an efficient tool to investigate the seismic capacity of URM structures [13-16]. This method does not pay much attention to the elastic strains which are only a small percentage of the total strain. In many cases, elastic strains can be totally neglected without important loss of accuracy and assuming that the structure comprises rigid bodies [17]. However, the dynamic nature of earthquakes is not equivalent with the static forces that can cause overturn of a structure. The dynamic response of a rigid body is investigated in many papers (e.g. [18, 19]). Limit analysis can tackle the complicated issue of the dynamic response of rigid bodies and give a simple solution regarding the capacity curve. The capacity curve is defined from the capacities in terms of both accelerations and displacements [20]. This curve can be assumed either bilinear or trilinear. In the following paragraphs, the methodology is explicitly applied to determine the bilinear capacity of the structure under investigation.

III. HISTORY OF THE MONUMENT

The campanile structure is a post-Byzantine tower which dates back to 1427 AD and is located on Mount Athos, in Chalkidiki, Greece. It is a slender structure 25.5m high, at the uppermost top of the sharp-angled roof (Fig. 1). The height of the masonry structure without the roof structure is 21.0m. The footprint of the tower is square with 5.5m side. Hence, the aspect ratio (i.e. the ratio of the width to the height) is 1/3.8. The width at the top of the structure is 5.25m which means that there is a decrease of 25cm and a deflection (from the verticality) 7‰.

Fig. 1 3D views of the structure

A. URM Piers

The piers of the structure are constructed from rubble URM carefully bonded. The angles are constructed with quarry-faced masonry where the beds and the sides are finely chisel-dressed, but faces are roughly worked. Timber beams are embedded at several levels of the structures to improve the connection between perpendicular walls.

B. Belfry

The belfry, i.e. the upper part of a bell tower enclosing the bells is shown in Fig. 2. It has four square piers, sized 90cm×90cm and four intermediate piers half of solid stone and half of URM. The hip roof is a wooden structure which still keeps the timber elements of the initial construction.

DOI: 10.5963/JCES0601002

Fig. 2 Belfry of the tower

C. Seismic Damage

At least two strong seismic events have hit the monument [21]. On July 28th 1585, according to historical evidence, a severe earthquake shook the Monastery and caused the partial collapse of the defense walls and other structures. It is very likely that this earthquake caused cracks at the base of the structure. This explanation is related to the fact that at this level there are several very old masonry infills. Indeed, in the case of cracking of the masonry a filling with masonry rubble can increase the stiffness of the structure.

During the second important earthquake of 1932, the belfry was damage, and a steel tie-rods structure was necessary to ensure the safety of the structure.

IV. MODAL CHARACTERISTICS OF THE MONUMENT

The modal characteristics of the tower are estimated using a finite element model (FEM) and the mechanical properties presented in Table 1 and carrying out a modal analysis. URM is neither a homogeneous nor an isotropic material. The assumed mechanical properties are an average of similar structures; for example, compressive strength is reported to vary between 2 to 4 MPa approximately [10, 22-35].

TABLE 1 MECHANICAL CHARACTERISTICS OF MASONRY [IN KN, M]

Compressive strength [kN/m^2]	**Tensile strength [kN/m^2]**	**Shear strength [kN/m^2]**	**Elastic modulus [kN/m^2]**	**Shear Modulus [kN/m^2]**	**Specific weight [kN/m^3]**
3,000	0	0	2.5×10^6	0.8×10^6	23

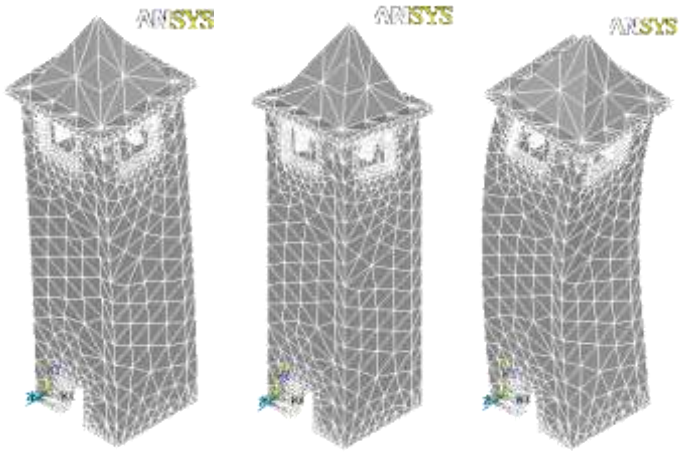

(a) (b) (c)

Fig. 3 The first three modal shapes: (a) translational mode 1, (b) translational mode 2, (c) twisting mode 3

DOI: 10.5963/JCES0601002

It is also known that URM is not an isotropic material [36, 37]; nevertheless, the difference in the strength in the two axis for a biaxial stress state is not high [38-44], and thus, URM may be assumed isotropic without significant loss of accuracy. ANSYS software is used to model the structure. Hexahedral elements are used for the tower and the roof. The mass is uniformly distributed. Given that the number of nodes is high, the number of modes is also high. However, not all of them are crucial but only those with a high participation mass ratio. The first three modes have an accumulated participation mass ratio more than 80%. The first modal frequency is 5.38Hz, the second one 5.50Hz, while the third one is 17.97Hz. The boundary conditions at the foundation level are assumed fixed and the masonry walls uncracked. These assumptions are quite conservative leading to high values for the modal frequencies. The first two modes have a translational shape in perpendicular axes, while the third one is mostly twisting about the vertical axis. The modal shapes are shown in Fig. 3.

V. COLLAPSE MECHANISMS

Collecting damage data about towers from recent earthquakes, it is possible to classify the recurrent types of collapse mechanisms. Damage data from the earthquakes of Friuli (1978) [45] and L'Aquila (2008) [46, 47], and Molise (2002) [48] show that there exist three main types of out-of-plane collapse mechanisms: (i) overturning of the tower, (ii) diagonal cracks and overturning of the critical part, and (iii) dislocation of the belfry. These collapse mechanisms are shown in Table 2.

TABLE 2 OUT-OF-PLANE COLLAPSE MECHANISMS

Designation	Collapse Mechanism	Out-of-plane damage
1 - ANA	Overturning	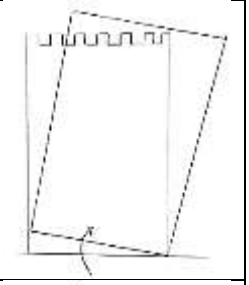
2 - DP	Diagonal cracking	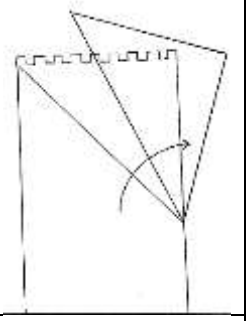
3 - KOP	Dislocation of the belfry	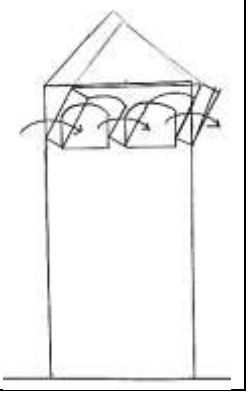

The methodology to estimate the capacity curve of the structure comprises four steps: three steps regarding the acceleration spectral capacity and one step for the displacement spectral capacity. The method is presented schematically in the following Fig. 4.

DOI: 10.5963/JCES0601002

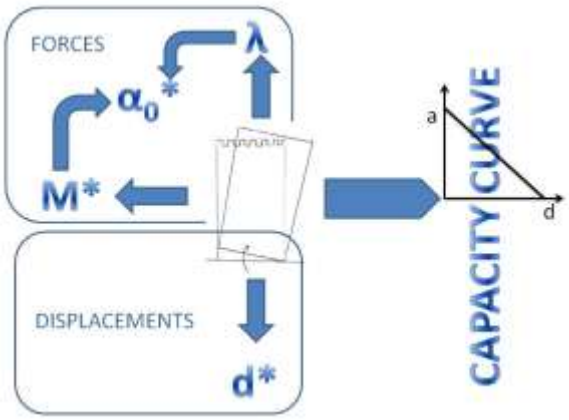

Fig. 4 Schematic representation of the limit analysis method

VI. ASSESSMENT BASED ON LIMIT ANALYSIS

A. *Acceleration-based Assessment*

The tower can be idealised with a simple rectangular structure shown in Fig. 5. At the top of the structure, there is an additional mass which represents the bells and the roof mass.

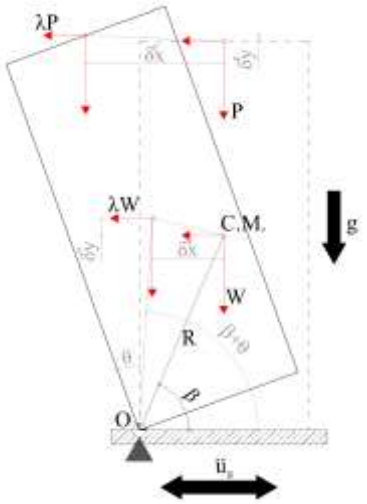

Fig. 5 Idealisation of the collapse mechanism

In this approach, the out-of-plane safety factor λ is estimated simulating the inertia effect with equivalent static forces [49, 50]. Regarding the first collapse mechanism (i = 1), the method is applied in the following steps:

1) Step 1: Estimation of Critical Static Safety Factor λ

The critical ratio λ of the horizontal actions needed to overturn the tower can be evaluated applying the principle of virtual works for an infinitesimal rotation dθ shown in Fig. 3 as follows:

$$\lambda = \frac{\sum_i W_{i,x}}{\sum_j W_{j,y}} = \frac{G\dot{\delta}_{y,G} + P\dot{\delta}_{y,P}}{G\dot{\delta}_{x,G} + P\dot{\delta}_{x,P}} \quad (1)$$

In the above Eq. 1, $W_{i,x}$ is the virtual work of the action i in the horizontal direction (x) and $W_{j,y}$ is the virtual work of the action j in the vertical direction (y). G is the gravity force concentrated at the center of gravity of the investigated part and P is the weight of the bells and the roof. $\delta_{i,j}$ is the displacement at the i direction ($i = x, y$) of the j action ($j = G, P$) while the dot over δ stands for the derivative of the respective displacement (i.e. an infinitesimal displacement).

Moment equilibrium would result in an equivalent relation with Eq. 1. It is found a λ equal to 0.34. This value represents the sufficient horizontal force needed to cause the onset of overturning ($\theta = 0^0$) of the tower under static conditions.

DOI: 10.5963/JCES0601002

2) Step 2: Determination of Equivalent SDOF

The transformation of the rocking rigid body into an equivalent SDOF system is necessary to perform the assessment using the response spectrum of the base motion. It should be noted that the equivalency applies as long as the rigid body tilts around the same pivot point. The restriction applies here as the rocking is only one sided. The mass of the rocking system is distributed along the height. The mass of the equivalent SDOF system is given by the following equation:

$$M^* = \frac{\left(\sum_{i=1}^{N} P_i \Delta_{x,i}\right)^2}{g\sum_{i=1}^{N} P_i \Delta_{x,i}^2} \tag{2}$$

In Eq. 2, the summation for the collapse mechanism is performed by the two components of the vertical load, i.e. the self-weight $P_1 = G$ of the tower and the hip roof and the bells $P_2 = P$. Eq. 2 represents the modal mass of the considered first mode which has $\Delta_{x,i} = \varphi_{1,i}$. Having assumed that the deformation of the wall is neglected which is a reasonable assumption for walls tilting around their base, all points are tilting by the same angle θ and the horizontal projection of the displacements $\Delta_{x,i}$ is linear along the height of the wall.

The effective modal mass is then found M^* = 202 ton. The effective mass ratio which is given by the next Eq. 3 is equal to 99%.

$$e^* = \frac{gM^*}{\sum_{i=1}^{N} P_i} \tag{3}$$

3) Step 3: Spectral Acceleration Capacity

The acceleration at the base of the equivalent SDOF system needed to initiate the rocking of the rigid body is given by the maximum value of coefficient λ normalized by the effective mass ratio according to the following expression:

$$a_0^* = \frac{\lambda}{e^*} \tag{4}$$

Eq. 4 results in a_0^* = 0.39g. In the force-based assessment, the spectral acceleration demand is estimated taking into account the substructure filtering effect and the subsequent NL response introducing, on the one hand, a behaviour factor q (or equivalently a reduction factor R) and the basic characteristics of the fundamental period of the underlying structure. The following expression is proposed by the Eurocode 8 [51]:

$$S_e^d(T) = \frac{S_e(T_1)}{q} \cdot \psi(Z) \cdot \gamma \tag{5}$$

In Eq. 5, ψ(Z) is the shape of the fundamental mode of vibration of the building in the direction considered, normalised to the displacement at the top of the building. A reasonable approximation of the fundamental mode of regular masonry buildings is given by the following expression in which H stands for the height of the structure measured from the foundation and Z stands for the height from the building foundation to the centre of gravity of the weight forces, whose masses generate horizontal forces on the elements of the kinematic chain and which are not efficiently transmitted to the other parts of the building respectively:

$$\psi(Z) = \frac{Z}{H} \tag{6}$$

The above Eq. 6 gives the value ψ(Z) = 21/25.5 = 0.82 where the structure is considered with a total height H = 25.5m which is the total height. In Eq. 5, γ is the corresponding modal participation factor given by the following expression [51]:

$$\gamma = \frac{3n}{2n+1} \tag{7}$$

In the above Eq. 7, n is the number of stories of the building. The tower is assumed as a one storey structure, and the participation factor takes the value γ = 1.0 whereas when assumed as n = 2 then, γ = 1.2. A q behaviour factor has been proposed for rocking bodies equal to 2 [51]. Using the above Eqs. 5, 6 and 7 and the EC-8 acceleration spectrum of Fig. 6 with PGA = 0.42g then, the spectral acceleration demand of the building is evaluated as S_{ad} = 0.43g. The resulting collapse safety factor equals to $\gamma_{R,a}$ = 91% showing marginal safety.

DOI: 10.5963/JCES0601002

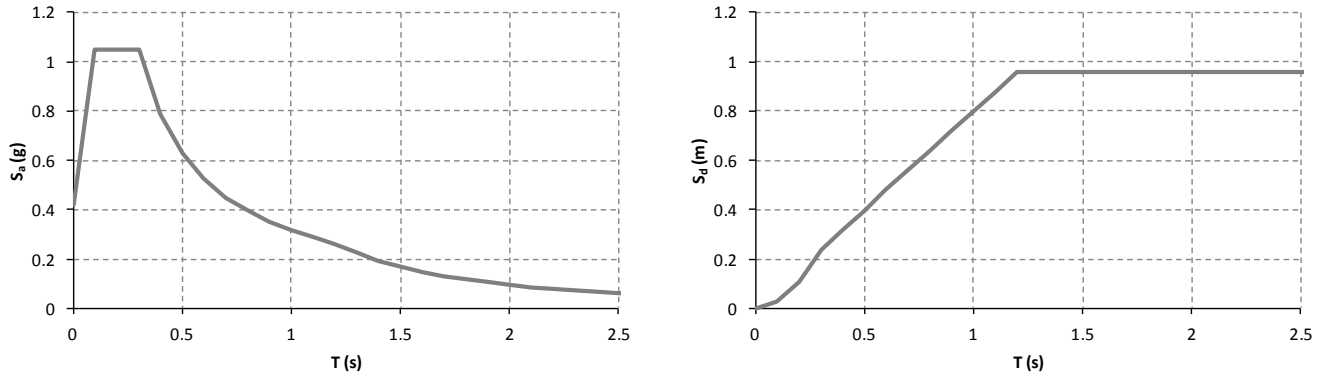

Fig. 6 Acceleration and displacement response spectra

B. Displacement-based Assessment

It is well known that a rocking pier possesses a dynamic reserve capacity when subjected to an out-of-plane transient loading. Therefore, the horizontal static multiplier itself is not sufficient to predict the dynamic capacity and hence, it is necessary to consider the transcendental nature of the seismic excitation.

The principle of virtual work (PVW) for an admissible displacement $\dot{\delta}$ is applied to evaluate the minimum value of a static horizontal multiplier of the vertical weights of the building $\boldsymbol{\lambda}$ that corresponds to the static threshold resistance. The $\boldsymbol{\lambda_{lim}}$ value is the safety factor of the potential horizontal loading that the structure can support, but for stresses satisfying a considered strength criterion. The local strength criterion is convex and based on a non-linear distribution of compression stresses with zero tensile strength. This lower bound scheme constitutes the following optimization problem of λ for Θ:

$$\min \lambda \,|\sum_{N}\left[\delta W(F_i)+\delta W(\lambda f_i)\right]=0 \tag{8}$$

The maximum value of λ represents the necessary inertia at the base of the rocking mechanism to initiate the rotation of the mechanism ($\theta \rightarrow 0$). Solving Eq. 2 for dθ when the system is about to rotate i.e. initiation of rotation - almost being at rest: limλ for $\theta \rightarrow 0$ and considering the forces appearing at the collapse mechanism shown in Fig. 3 a λ equal to 0.43 is found for the respective mechanism. This value is equivalent to the horizontal static forces needed to overturn the tower under the current configuration.

As the rotation θ is going increasingly high, λ will drop to zero. This instant represents the ultimate condition for rocking of the mechanism and sets off the collapse state due to overturning.

The maximum rotation θ of the vibrating tower before collapse should be calculated from Eq. 1 for $\lambda = 0$. This value is found equal to θ_{ult} = 0.325rad for the collapse mechanism through an iterative procedure consisting of a stepwise gradual increase of $\dot{\delta}$ and estimating the resulting λ. The maximum top displacement for $\lambda = 0$ is then, derived equal to $d_{k,0}$ = 4.71m for the overturning of the tower.

The displacement-based assessment consists in comparing the ultimate displacement capacity d^*_u of the equivalent SDOF system of the local mechanism and the displacement demand Δ_d from the displacement spectrum estimated with respect to the secant period T_s. Using a standard modal analysis procedure, the displacement capacity d^* for the equivalent SDOF results from the top displacement of the mechanism multiplied by the inverted modal participation factor of the first mode $(\Gamma_1)^{-1}$ applying the following expression similar to Eq. 4 for mass:

$$d^* = d_k \frac{\sum_{i=1}^{n+m} P_i \Delta_{x,i}^2}{\Delta_{x,k} \sum_{i=1}^{n+m} P_i \Delta_{x,i}} = d_k \frac{\Gamma_1^{-1}}{\Delta_{x,k}} \tag{9}$$

In the above Eq. 9, d_k is the relative displacement to the base of the mechanism at the control point of the collapse mechanism and $\Delta_{x,i}$ are the virtual horizontal displacements of the various weights P_i. These displacements are considered equivalent to modal displacements and are normalized against the top modal displacement value (i.e. $\Delta_{x,k}$). The maximum displacement $d_{k,0}$ that the mechanism can sustain is calculated from Eq. 1 for $\lambda = 0$. The SDOF coefficient of Eq. 9, i.e. the normalised modal participation factor $\Gamma^{-1}/\Delta_{x,k}$, is equal to 0.50 for the overturning of the tower. The maximum displacement of the equivalent SDOF system d_0^* would be 2.37m. The resulting capacity curve for collapse mechanism is presented in Fig. 7. It is seen that the capacity curve is bilinear with the second branch having a constant negative slope.

DOI: 10.5963/JCES0601002

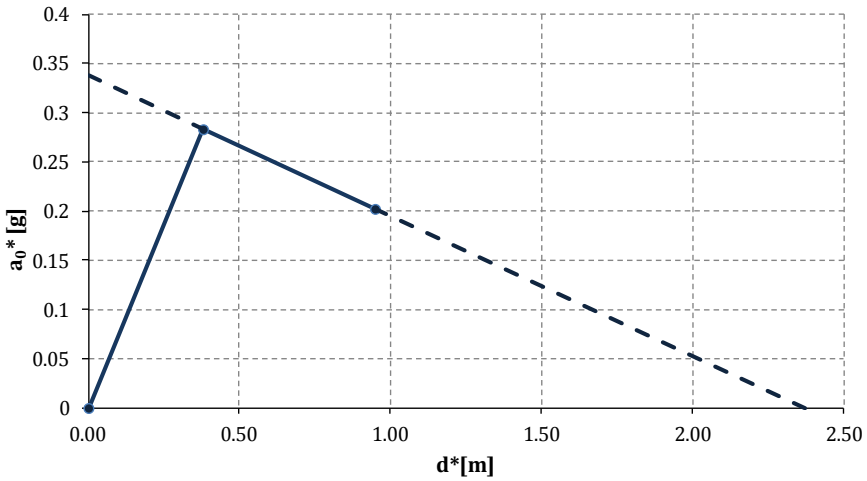

Fig. 7 Capacity curve

Comparisons with NL analyses and experimental results have shown that the maximum displacement of the equivalent SDOF system d_0^* should be reduced by 40-50% [8, 52]. In this mechanism the reduction would result in an ultimate displacement of the collapse mechanism (40%) $d_0^* = d_u^* = 0.95$m. Obviously, this value is very high, but given the modelling assumptions (i.e. rigid body rotation) it should be expected. Given that the height of the structure is 25.5 m, the ultimate displacement corresponds to a drift capacity at the ultimate state of this collapse mechanism equal to $\theta_u = 3.7\%$. Drift capacities exceeding 6% for URM rocking walls have been measured experimentally [53]. However, this value reveals that this mechanism is not very likely to be the critical one.

The equivalent SDOF systems with the capacity curve shown in Fig. 7 is not characterized by a unique natural frequency as their non-linear response suggests. However, these non-linear systems can be idealised with an equivalent linear SDOF system with an effective natural period which maximizes the response [14]. This appears in a fraction of the ultimate displacement which according to [10] is at the 40% of the ultimate displacement. Once the effective displacement $d_s^* = 0.4 d_u^*$ is estimated (0.38m) and, the effective acceleration corresponding to the effective displacement d_s^* is identified on the capacity curve ($a_s^* = 0.28g = 2.75 m/s^2$) the effective secant period Ts is calculated using the secant properties of the equivalent SDOF elastic system ([54, 55]):

$$T_s = 2\pi\sqrt{\frac{M^*}{K^*}} = 2\pi\sqrt{\frac{d_s^*}{a_s^*}} \tag{10}$$

The effective secant period is found 2.32s. The natural period of the building has been estimated experimentally equal to $T_1 = 0.19$s before the non-linear response of the structure due to rocking. The ratio between the natural periods T_s / T_1 is 13.46.

VII. COMPARISON

The displacement demand for the structure is estimated using the displacement response spectrum of Fig. 6 and the effective secant period. The displacement demand results in $S_d = 0.95$m while the displacement capacity is found $d_u^* = 0.95$m. Hence, the displacement safety factor is equal to $\gamma_{R,d} = 100\%$.

The respective force safety factor was found equal to $\gamma_{R,a} = 91\%$ which would result in a marginal collapse. However, the monument stands for six centuries without any collapse showing that the displacement assessment leads to more accurate results.

The values of the static horizontal forces multiplier λ and the ultimate displacement capacity found reasonably comparable with other case studies [56, 57].

VIII. CONCLUSIONS

A monument erected in the 15th century is investigated. The tower was built to host the bells of the monastery. An investigation of the structure revealed damaged parts which can be connected to strong earthquakes that hit the monument in the past. The rocking response due to seismic action is examined. The application of two assessment methodologies, a force-based and a displacement-based, gives robust results. Both methods are based on the limit analysis and assume that the structure behaves as a semi-rigid body and on the other hand, the cracks are already known. Obviously, neither of them is totally accurate. Within reasonable bounds, both can give a good estimate of the capacity of the structure with the latter being quite accurate in the prediction of the capacity while the former appears more conservative. Their accuracy depends on the

DOI: 10.5963/JCES0601002

respective accuracy of the assumptions.

Given the simplified model and the total uncertainties of the limit analysis procedure, the safety estimate should be applied with certain caution when the force based assessment is used while the estimates of the demands and the capacity of each collapse mechanism are rather consistent for the displacement based assessment.

ACKNOWLEDGMENT

The author gratefully acknowledges the financial support to carry out this research provided by IKY Fellowships of Excellence for Postgraduate Studies in Greece - Siemens Program.

REFERENCES

[1] T. M. Ferreira, A. A. Costa, and A. Costa, "Analysis of the out-of-plane seismic behavior of unreinforced masonry: A Literature Review," *International Journal of Architectural Heritage*, vol. 9, no. 8, pp. 949-972, 2014.

[2] L. Landi, R. Gabellieri, and P. P. Diotallevi, "A model for the out-of-plane dynamic analysis of unreinforced masonry walls in buildings with flexible diaphragms," *Soil Dyn. Earthq. Eng.*, vol. 79, pp. 211-222, Dec. 2015.

[3] D. P. Abrams, "Response of unreinforced masonry buildings," *J. Earthq. Eng.*, vol. 1, no. 1, pp. 257-273, Jan. 1997.

[4] F. Portioli, C. Casapulla, L. Cascini, M. D'Aniello, and R. Landolfo, "Limit analysis by linear programming of 3D masonry structures with associative friction laws and torsion interaction effects," *Arch. Appl. Mech.*, vol. 83, no. 10, pp. 1415-1438, 2013.

[5] M. J. Kowalsky, M. J. N. Priestley, and G. A. MacRae, "Displacement-based design of RC bridge columns in seismic regions," *Earthq. Eng. Struct. Dyn.*, vol. 24, no. 12, pp. 1623-1643, 1995.

[6] J. P. Moehle, "Displacement-based design of RC structures subjected to earthquakes," *Earthq. Spectra*, vol. 8, no. 3, pp. 403-428, 1992.

[7] M. J. N. Priestley, G. M. Calvi, and M. J. Kowalsky, *Displacement-based Seismic Design of Structures*, vol. 17, IUSS Press, Pavia, Italy, 2007.

[8] S. Lagomarsino, "Seismic assessment of rocking masonry structures," *Bull. Earthq. Eng.*, vol. 13, no. 1, pp. 97-128, 2014.

[9] G. Milani, P. Lourenço, and A. Tralli, "Homogenization approach for the limit analysis of out-of-plane loaded masonry walls," *J. Struct. Eng.*, vol. 132, no. 10, pp. 1650-1663, 2006.

[10] A. Giordano, A. De Luca, E. Mele, and A. Romano, "A simple formula for predicting the horizontal capacity of masonry portal frames," *Eng. Struct.*, vol. 29, no. 9, pp. 2109-2123, 2007.

[11] N. T. K. Lam, M. Griffith, J. Wilson, and K. Doherty, "Time-history analysis of URM walls in out-of-plane flexure," *Eng. Struct.*, vol. 25, no. 6, pp. 743-754, 2003.

[12] M. Indirli, L. A. S. Kouris, A. Formisano, R. P. Borg, and F. M. Mazzolani, "Seismic damage assessment of unreinforced masonry structures after the Abruzzo 2009 earthquake: The case study of the historical centers of L'Aquila and Castelvecchio Subequo," *Int. J. Archit. Herit.*, vol. 7, no. 5, pp. 536-578, 2013.

[13] D. Theodossopoulos and B. Sinha, "A review of analytical methods in the current design processes and assessment of performance of masonry structures," *Constr. Build. Mater.*, vol. 41, no. 2, pp. 990-1001, 2013.

[14] H. Alexakis and N. Makris, "Limit equilibrium analysis and the minimum thickness of circular masonry arches to withstand lateral inertial loading," *Arch. Appl. Mech.*, vol. 84, no. 5, pp. 757-772, 2014.

[15] P. Roca, F. López-Almansa, J. Miquel, and A. Hanganu, "Limit analysis of reinforced masonry vaults," *Eng. Struct.*, vol. 29, no. 3, pp. 431-439, 2007.

[16] G. De Felice, "Out-of-plane seismic capacity of masonry depending on wall section morphology," *Int. J. Archit. Herit.*, vol. 5, no. 4-5, pp. 466-482, 2011.

[17] J. Heyman, "The stone skeleton," *Int. J. Solids Struct.*, vol. 2, no. 2, pp. 249-256-NaN-264-NaN-279, 1966.

[18] G. W. Housner, "The behavior of inverted pendulum structures during earthquakes," *Bull. Seismol. Soc. Am.*, vol. 53, no. 2, pp. 403-417, 1963.

[19] E. G. Dimitrakopoulos and M. J. DeJong, "Revisiting the rocking block: closed-form solutions and similarity laws," *Proc. R. Soc. A Math. Phys. Eng. Sci.*, vol. 468, no. 2144, pp. 2294-2318, Apr. 2012.

[20] K. Doherty, M. C. Griffith, N. Lam, and J. Wilson, "Displacement-based seismic analysis for out-of-plane bending of unreinforced masonry walls," *Earthq. Eng. Struct. Dyn.*, vol. 31, no. 4, pp. 833-850, 2002.

[21] B. Papazachos and C. Papazachou, *The Earthquakes of Greece*, Ziti Editions publications, Thessaloniki, Greece, 304 pp., 1997.

[22] F. V Karantoni and M. N. Fardis, "Effectiveness of seismic strengthening techniques for masonry buildings," *J. Struct. Eng.*, vol. 118, no. 7, pp. 1884-1902, 1992.

[23] L. Binda, J. Pina-Henriques, A. Anzani, A. Fontana, and P. B. Lourenço, "A contribution for the understanding of load-transfer mechanisms in multi-leaf masonry walls: testing and modelling," *Eng. Struct.*, vol. 28, no. 8, pp. 1132-1148, 2006.

[24] A. Doğangün, H. Sezen, Ö. İskender Tuluk, R. Livaoğlu, and R. Acar, "Traditional Turkish masonry monumental structures and their earthquake response," *Int. J. Archit. Herit.*, vol. 1, no. 3, pp. 251-271, 2007.

[25] A. Bayraktar, N. CoŞkun, and A. Yalçin, "Damages of masonry buildings during the July 2, 2004 Doğubayazit (Ağri) earthquake in Turkey," *Eng. Fail. Anal.*, vol. 14, no. 1, pp. 147-157, 2007.

[26] D. Benedetti, P. Carydis, and M. P. Limongelli, "Evaluation of the seismic response of masonry buildings based on energy functions," *Earthq. Eng. Struct. Dyn.*, vol. 30, no. 7, pp. 1061-1081, 2001.

DOI: 10.5963/JCES0601002

[27] E. Vintzileou and A. Miltiadou-Fezans, "Mechanical properties of three-leaf stone masonry grouted with ternary or hydraulic lime-based grouts," *Eng. Struct.*, vol. 30, no. 8, pp. 2265-2276, 2008.

[28] T. F. Paret, S. A. Freeman, G. R. Searer, M. Hachem, and U. M. Gilmartin, "Using traditional and innovative approaches in the seismic evaluation and strengthening of a historic unreinforced masonry synagogue," *Eng. Struct.*, vol. 30, no. 8, pp. 2114-2126, 2008.

[29] A. Penna, "Seismic assessment of existing and strengthened stone-masonry buildings: critical issues and possible strategies," *Bull. Earthq. Eng.*, vol. 13, no. 4, pp. 1051-1071, Aug. 2014.

[30] P. B. Lourenço and L. F. Ramos, "Characterization of cyclic behavior of dry masonry joints," *J Struct Eng*, vol. 130, no. 5, pp. 779-786, 2004.

[31] A. A. Costa, A. Arêde, A. Costa, J. Guedes, and B. Silva, "Experimental testing, numerical modelling and seismic strengthening of traditional stone masonry: comprehensive study of a real Azorian pier," *Bull. Earthq. Eng.*, pp. 1-25, 2010.

[32] B. Villemus, J. C. Morel, and C. Boutin, "Experimental assessment of dry stone retaining wall stability on a rigid foundation," *Eng. Struct.*, vol. 29, no. 9, pp. 2124-2132, 2007.

[33] C. Calderini, S. Cattari, and S. Lagomarsino, "In-plane strength of unreinforced masonry piers," *Earthq. Eng. Struct. Dyn.*, vol. 38, no. 2, pp. 243-267, 2009.

[34] S. S. Kouris, "Applied earthquake engineering in the research of vulnerable masonry structures," *J. Civ. Eng. Sci.*, vol. 1, no. 4, pp. 39-46, 2012.

[35] S. S. Kouris and M. K. K. Weber, "Numerical analysis of masonry bell-towers under dynamic loading," *J. Civ. Eng. Archit.*, vol. 5, no. 8, pp. 715-722, 2011.

[36] A. A. Hamid and R. G. Drysdale, "Proposed failure criteria for concrete block masonry under biaxial stresses," *ASCE J Struct Div*, vol. 107, no. 8, pp. 1675-1687, 1981.

[37] R. G. Drysdale, A. A. Hamid, and L. R. Baker, *Masonry Structures: Behavior and Design*, Prentice Hall, 1994.

[38] A. W. Page, "Biaxial compressive strength of brick masonry," *Proc. Inst. Civ. Eng. (London). Part 1 - Des. Constr.*, vol. 71, no. pt 2, pp. 893-906, 1981.

[39] M. Dhanasekar, A. W. Page, and P. W. Kleeman, "Failure of brick masonry under biaxial stresses," *Proc. Inst. Civ. Eng.*, vol. 79, no. pt 2, pp. 295-313, 1985.

[40] K. Naraine and S. Sinha, "Stress-strain curves for brick masonry in biaxial compression," *J. Struct. Eng.*, vol. 118, no. 6, pp. 1451-1461, 1992.

[41] M. Dhanasekar, P. W. Kleeman, and A. W. Page, "Biaxial stress-strain relations for brick masonry," *J. Struct. Eng.*, vol. 111, no. 5, pp. 1085-1100, 1985.

[42] K. Naraine and S. Sinha, "Cyclic behavior of brick masonry under biaxial compression," *J. Struct. Eng.*, vol. 117, no. 5, pp. 1336-1355, 1991.

[43] H. R. Ganz and B. Thürlimann, "Tests on the biaxial strength of masonry," *Tech. Rep. No.7502*, vol. 3, 1982.

[44] A. Bernardini, C. Modena, and U. Vescovi, "An anisotropic biaxial failure criterion for hollow clay brick masonry," *Int. J. Masonry Constr.*, vol. 2, no. 4, p. 165, 1982.

[45] V. Kárník, D. Procházková, Z. Schenková, L. Ruprechtová, A. Dudek, J. Drimmel, E. Schmedes, G. Leydecker, J. P. Rothé, B. Guterch, H. Lewandowska, D. Mayer-Rosa, D. Cvijanović, V. Kuk, F. Giorgetti, G. Grünthal, and E. Hurtig, "Map of isoseismals of the main Friuli earthquake of 6 May 1976," *Pure Appl. Geophys.*, vol. 6, pp. 1307-1313, 1978.

[46] A. Formisano, M. R. Grippa, P. Di Feo, and G. Florio, "L'Aquila earthquake: a survey in the historical centre of Castelvecchio Subequo," in *Proc. of the COST Action C26 Final Conference "Urban Habitat Constructions under Catastrophic Events"*, 2010, vol. 1, pp. 371-376.

[47] D. Bindi, F. Pacor, L. Luzi, M. Massa, and G. Ameri, "The Mw 6.3, 2009 L'Aquila earthquake: Source, path and site effects from spectral analysis of strong motion data," *Geophys. J. Int.*, vol. 179, no. 3, pp. 1573-1579, 2009.

[48] L. D. Decanini, A. De Sortis, A. Goretti, L. Liberatore, F. Mollaioli, and P. Bazzurro, "Performance of masonry buildings during the 2002 Molise, Italy, earthquake," *Earthq. Spectra*, vol. 20, no. S1, pp. S191-S220, 2004.

[49] D. P. Abrams, R. Angel, and J. Uzarski, "Out-of-plane strength of unreinforced masonry infill panels," *Earthq. Spectra*, vol. 12, no. 4, pp. 825-844, 1996.

[50] R. D. Ewing and J. C. Kariotis, "Methodology for mitigation of seismic hazards in existing unreinforced masonry buildings: Wall testing, out-of-plane," *Methodology for Mitigation of Seismic Hazards in Existing Unreinforced Masonry Buildings: Diaphragm Testing*, ABK, El Segundo, CA, Technical report 04, 1981.

[51] CEN, "Eurocode 8, design of structures for earthquake resistance. Part 1: general rules, seismic actions and rules for buildings," *Eur. Stand. NF EN*, vol. 1, 1998.

[52] M. C. Griffith, G. Magenes, G. Melis, and L. Picchi, "Evaluation of out-of-plane stability of unreinforced masonry walls subjected to seismic excitation," *Journal of Earthquake Engineering*, vol. 7(sup1), pp. 141-169, 2003.

[53] S. Lagomarsino, "On the vulnerability assessment of monumental buildings," *Bull. Earthq. Eng.*, vol. 4, no. 4, pp. 445-463, 2006.

[54] P. Fajfar, "Capacity spectrum method based on inelastic demand spectra," *Earthq. Eng. Struct. Dyn.*, vol. 28, no. 9, pp. 979-994, 1999.

[55] P. Fajfar, "A nonlinear analysis method for performance-based seismic design," *Earthq. Spectra*, vol. 16, no. 3, pp. 573-592, 2000.

[56] F. Peña, P. B. Lourenço, N. Mendes, and D. V Oliveira, "Numerical models for the seismic assessment of an old masonry tower," *Eng. Struct.*, vol. 32, no. 5, pp. 1466-1478, 2010.

[57] A. Preciado, S. T. Sperbeck, and A. Ramírez-Gaytán, "Seismic vulnerability enhancement of medieval and masonry bell towers externally prestressed with unbonded smart tendons," *Eng. Struct.*, vol. 122, pp. 50-61, 2016.

DOI: 10.5963/JCES0601002